Article

Rampant Arch and Its Optimum Geometrical Generation

Cristina Velilla [1], Alfredo Alcayde [2] , Carlos San-Antonio-Gómez [1], Francisco G. Montoya [2] , Ignacio Zavala [1] and Francisco Manzano-Agugliaro [2,*]

[1] Department of Ingeniería Agroforestal, Universidad Politécnica de Madrid, Av. De Puerta de Hierro, 28040 Madrid, Spain; cristina.velilla@upm.es (C.V.); c.sanantonio@upm.es (C.S.-A.-G.); ignacio.zavala.morencos@upm.es (I.Z.)

[2] Department of Engineering, University of Almeria, ceiA3, 04120 Almeria, Spain; aalcayde@ual.es (A.A.); pagilm@ual.es (F.G.M.)

*   Correspondence: fmanzano@ual.es; Tel.: +34-950-015396; Fax: +34-950-015491

check for updates

Abstract: Gothic art was developed in western Europe from the second half of the 12th century to the end of the 15th century. The most characteristic Gothic building is the cathedral. Gothic architecture uses well-carved stone ashlars, and its essential elements include the arch. The thrust is transferred by means of external arches (flying buttresses) to external buttresses that end in pinnacles, which accentuates the verticality. The evolution of the flying buttresses should not only be considered as an aesthetic consideration, but also from a constructive point of view as an element of transmission of forces or loads. Thus, one evolves from a beam-type buttress to a simple arch, and finally to a rampant arch. In this work, we study the geometry of the rampant arch to determine which is the optimum from the constructive point of view. The optimum rampant arch obtained is the one with the common tangent to the two arches parallel to the slope line. A computer program was created to determine this optimal rampant arch by means of a numerical or graphical input. It was applied to several well-known and representative cases of Gothic art in France (church of Saint Urbain de Troyes) and Spain (Cathedral of Palma de Mallorca), establishing if they were designs of optimal rampant arches or not.

Keywords: rampant arch; geometry; optimum; flying buttresses; cathedral

1. Introduction

The rampant arch is an arch whose starts, in walls or buttresses, are located at different levels, often with a considerable difference in height [1]. It was used extensively in Gothic architecture to shape the buttress, and its function was to transmit the thrust of the vaults to the buttresses and these to the foundations [2]. In addition to this structural function, the buttress serves to carry rainwater from the vaults [3] to the exterior through the pinnacles.

The most common rampant arch used in the flying buttresses of most well-known Gothic cathedrals is the one formed by a single circumferential arch [4]. According to Viollet-le-Duc (1854) [5] there are two types: flying buttresses in which the center of the circumference is in the wall (Figure 1A), and flying buttresses in which its center is displaced toward the interior of the building (Figure 1B). The first are the oldest flying buttresses, while the second are the most used because, from a mechanical point of view, they perform better than the first [6].
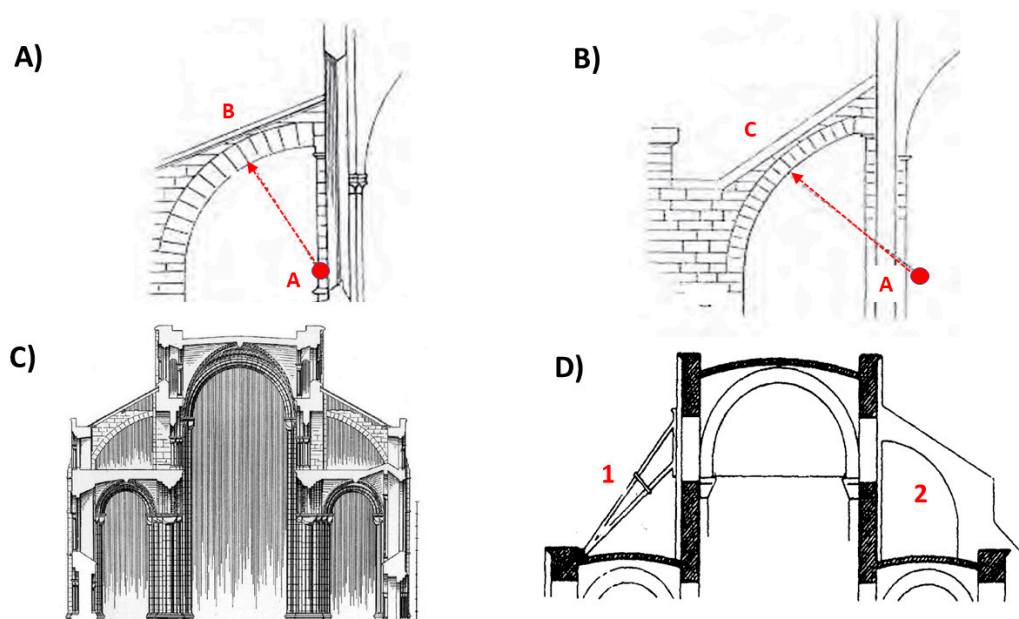
Figure 1. (**A**,**B**) The two types of flying buttresses according to Viollet-le-Duc [5]. (**C**) Section of Durham Cathedral [7]. (**D**) Wooden props from the vault of the church of Vézelay (1) replaced by stone flying buttresses (2) [8].

The flying buttresses appeared for the first time in Durham Cathedral around the year 1100 as an evolution of the hidden buttress in the triforium, where an opening is made that allows a longitudinal route parallel to the main nave [9]. In Durham, the buttress did not yet have the function of balancing the lateral thrusts of the vaults; its mission was to support the roof that covers the triforium (Figure 1C).

The flying buttresses of a single circumferential arch could also have been the result of the evolution of the framework of auxiliary wooden constructions that, from a certain moment on, appeared to support the Romanesque barrel vaults that were beginning to open up. Over time, these frameworks would begin to be built in stone (Figure 1D). This moment perhaps occurred in France at the Abbey of Vézelay [8], where the buttress would not be an "invention ex novo" but the evolution of those wooden structures known throughout France [10].

The rampant arch of a single circumferential arch played an essential role in the structural and formal conception of Gothic architecture, creating in the external volume of the cathedrals a succession of dematerialized planes composed of one, two, and even three rows of buttresses, contributing to the spatial richness of the building [11]. The successive rhythm of the flying buttresses and buttresses with their pinnacles of reinforcement makes it possible to open large windows with stained-glass windows that give great luminosity to the interior of the cathedral and give symbolic and immaterial value to the Gothic architecture, which contrasts with the heaviness of the Romanesque architecture it replaced (Figure 1D) [12].

Although the single-arch flying buttresses are usually used in large cathedrals, there are also flying buttresses made up of two circumferential arches (Figure 2A). In this case, the rampant arch results from the union of two circumferential arches, tangent in the key, whose centers are at different levels, so that their outcrops in the walls or buttresses are at different heights. Examples that could be cited include, in France, the flying buttresses of the Church of Saint Urbain de Troyes [13] (Figure 2B), where the red points (A and C) are the starting points of the two arches, and between which the unevenness of the flying buttress must be bridged, and those of the Cathedral of Beauvais, which alternate a first line of ramps of a single arch of circumference with another of two arches (Figure 3A) [14]. In Spain, for example, there are the original flying buttresses of the cathedral of Palma de Mallorca, made up of two rampant arches of one and two circumferential arches, integrated into a single flying buttress (Figure 3B) [15]. The rampant arches consisting of two circumferential arches are used in Gothic

architecture to shape the flying buttresses, but also to build stairs. In Spain, there are many examples such as the Monastery of Uclés in Cuenca (Figure 3C), in the palaces of the Generalitat de Barcelona and Valencia, and, in the latter city, the Lonja staircase (Figure 3D).
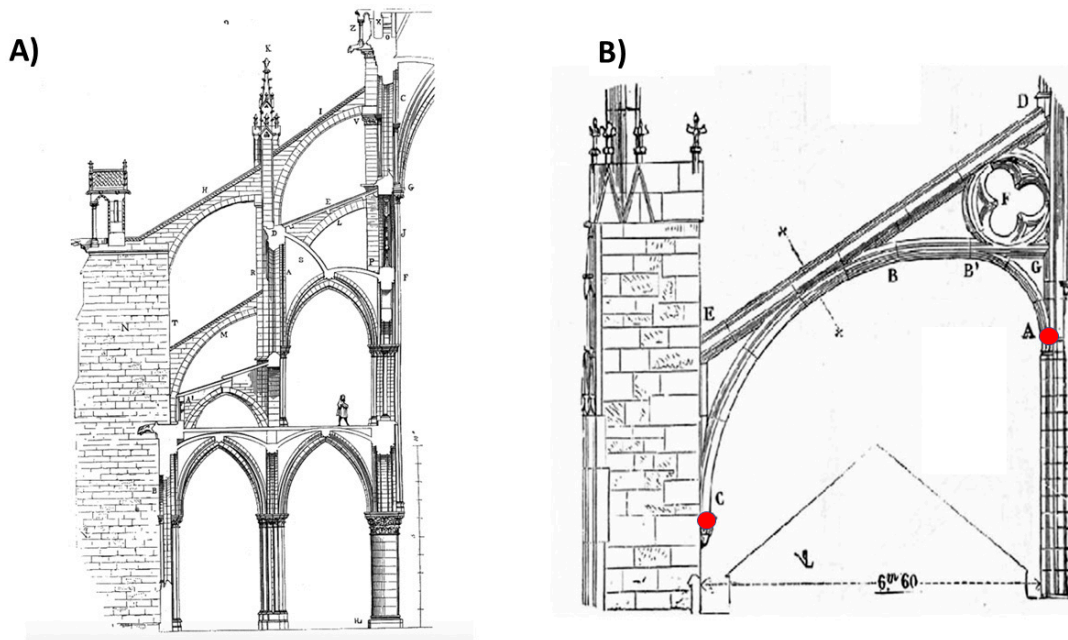
Figure 2. (**A**) Flying buttresses of Notre Dame (Paris) [5]. (**B**) Flying buttress of the church of Saint Urbain de Troyes [8].

Figure 3. (**A**) One- and two-arch circumference flying buttresses of Beauvais Cathedral (France). (**B**) Flying buttresses of the Cathedral of Palma de Mallorca. (**C**) Rampant arch in the staircase of the Monastery of Uclés (Cuenca). (**D**) Rampant arch in the staircase of La Lonja (Valencia).

The rampant arches were used profusely again at the end of the 19th century with the appearance of neo-Gothic architecture. Many churches were built throughout Europe, especially in France. In America, for example, cathedrals such as New York or Washington were built in the United States (Figure 4). In the same way, in modernism, these arches were also used.

**Figure 4.** Washington cathedral and its flying buttresses.

In general, the design of a rampant arch of a single arch does not present any difficulty, but the most difficult are the rampant arches of two arches, which throughout history were calculated graphically, and there is no consensus on which the optimal rampant arch of two arches is. The objectives of this work are to review the state of the art in the execution of rampant arches of two arches, to define which is the optimal one, to calculate the numerical solution, and to program it for its calculation and verification of rampant arches of already existing arches. As an additional objective, this work seeks to determine the starting points of the arches in the construction of the rampant arch.

2. Rampant Arches of Two Arches Graphically Constructed

The Gothic buildings raised the question of what methods were used by the builders in the design of their structures. The answer is that the Gothic builders had no method, only a great structural intuition nourished by the experience of successive collapses of structures. In classical texts, there are "structural rules" for dimensioning walls, pillars, and abutments of Gothic churches, all based on the

proportionality of the elements. These rules were applied or calculated using geometric or graphical constructions; see, for instance, treaties of Derand [16] or the later one of Blondel [17].

Thus, the usual for the execution of rampant arches was graphical construction, in which two cases were distinguished depending on which parameters were known (see Figure 5).
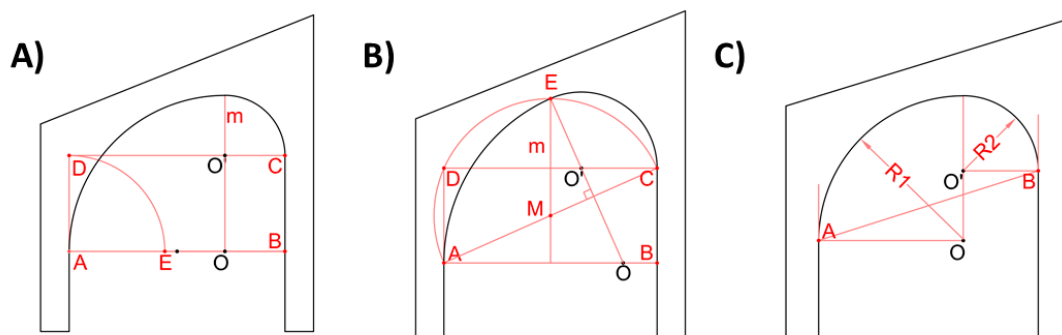
Figure 5. Rampant arches of two arches graphically constructed: (**A**) known A and C (method 1); (**B**) known A and C (method 2); (**C**) known radii of the two arcs ($R1$ and $R2$).

2.1. Rampant Arch 1: Known A and C (Starting of the Two Arches)

2.1.1. Method 1

In Figure 5A, the graphical drawing of the rampant arch is described, with the initial (A) and final (C) points known, where the tracing can be summarized as follows:

a.　The ABCD rectangle is drawn;
b.　With center in A, circumference of $R = AD$, obtaining E;
c.　Mediatrix m of BE is drawn;
d.　The intersection of m with the rectangle determines centers O and O'.

2.1.2. Method 2

In Figure 5B, the graphical drawing of the rampant arch is described, with the initial (A) and final (C) points known. Note that the centers are no longer parallel to the support pillars, where the tracing can be summarized as follows:

a.　The ABCD rectangle is drawn;
b.　Mediatrix m of AB determines M;
c.　With center in M, circumference of diameter AC is drawn;
d.　The intersection of this circumference with m is E;
e.　The perpendicular by E to AC determines the centers O and O'.

2.2. Rampant Arch 2: The Radii of the Two Arcs (R1 and R2) Are Known

In this other method, the radii of the two arcs ($R1$ and $R2$) are known, which add up the horizontal distance between both points, and it is a question of determining the centers of both.

1.　$R1 + R2$ = horizontal distance between both points (span);
2.　In A and B, perpendicular to the pillars where they are taken, $R1$ and $R2$ are used to obtain the centers O and O', respectively, of the arches.

3. The Optimal Rampant Arch

In the literature, there are different points of view for the optimal rampant arch. For example, there are studies that define it from the aesthetic point of view, or from a more harmonious view, in which

the curvatures of the different arches that compose it were more similar; here, the optimal rampant arch corresponds to the one in which the ratio between the curvatures of the lateral circumference and the central circumference is closer to one [18].

However, the rampant arch, apart from its aesthetic consideration, as explained in the introduction, has a structural load transmission function, as it replaces the function of a beam [19]. In addition, however, loads can only be transmitted by compression, as this is how the masonry resists bending moments and, therefore, sets the limits of the resistance capacity of the arches [20]. Figure 6 shows examples of classical studies concerned with this issue, i.e., the possible breaking points of rampant arches [21,22]. In this sense, classical research attempted to find the minimum value of "h" (the rise) for which masonry is able to withstand bending moments without any tensile strength [23], estimated to be between 3 and 5 tons of passive horizontal thrust. The optimum rampant arch, from the point of view of the support function or the transmission of the constructive loads, is the one in which the tangent common to the two circles that compose the arch is parallel to the straight unevenness between the points.
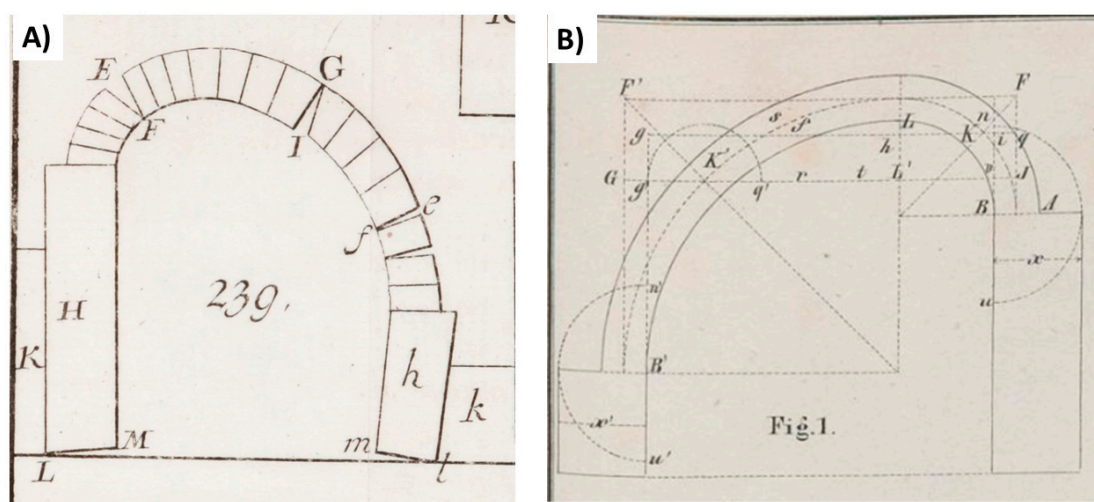
Figure 6. Classical studies of the rupture of rampant arches: (**A**) breakage of masonry by Frezier (1737) [21]; (**B**) calculation of the trust line by Breymann (1881) [22].

Note that there are examples where an inadequate intervention in the structure caused the fall of the dome or the vault, e.g., at Edinburgh in 1768, where the church of Holyrood Abbey collapsed after an inappropriate intervention in the vaults, where the essential buttressing system was rampant arches abutting the nave vault and their pier buttresses were capped with stabilizing pinnacles [24].

3.1. Graphical Design

This section describes the graphic drawing of an optimum rampant arch, i.e., the one whose tangent common to the two arches is parallel to the straight unevenness. The main ideas are as follows:

1. Once the gradient "d" is defined, which indicates the slope of a flying buttress or, where appropriate, of a staircase, the start of the arches is determined by points A and B, which are on a line parallel to "d".
2. Assuming the problem is solved, centers O and O' are on the straight perpendicular to the gradient line "d". In addition, O and O' are on the horizontal straight lines from A and B.
3. If from B, the line BC is drawn perpendicular to "d", where logically BC = OO'.
4. At this point, the question is reduced to place a segment OO' on the bisectors of the angles in M and N.

Thus, the graphical construction of Figure 7 was as follows:

a.   Any PQ line was drawn parallel to "d".
b.   The bisectors b_1 and b_2 of the angles were in P and Q.
c.   BC was traced perpendicular to "d".
d.   BC was moved (by parallelism) until the TS = BC segment was obtained on the bisectors.
e.   TS was moved (by parallelism on the perpendicular to AC) to points O and O', which are the centers of the arches.
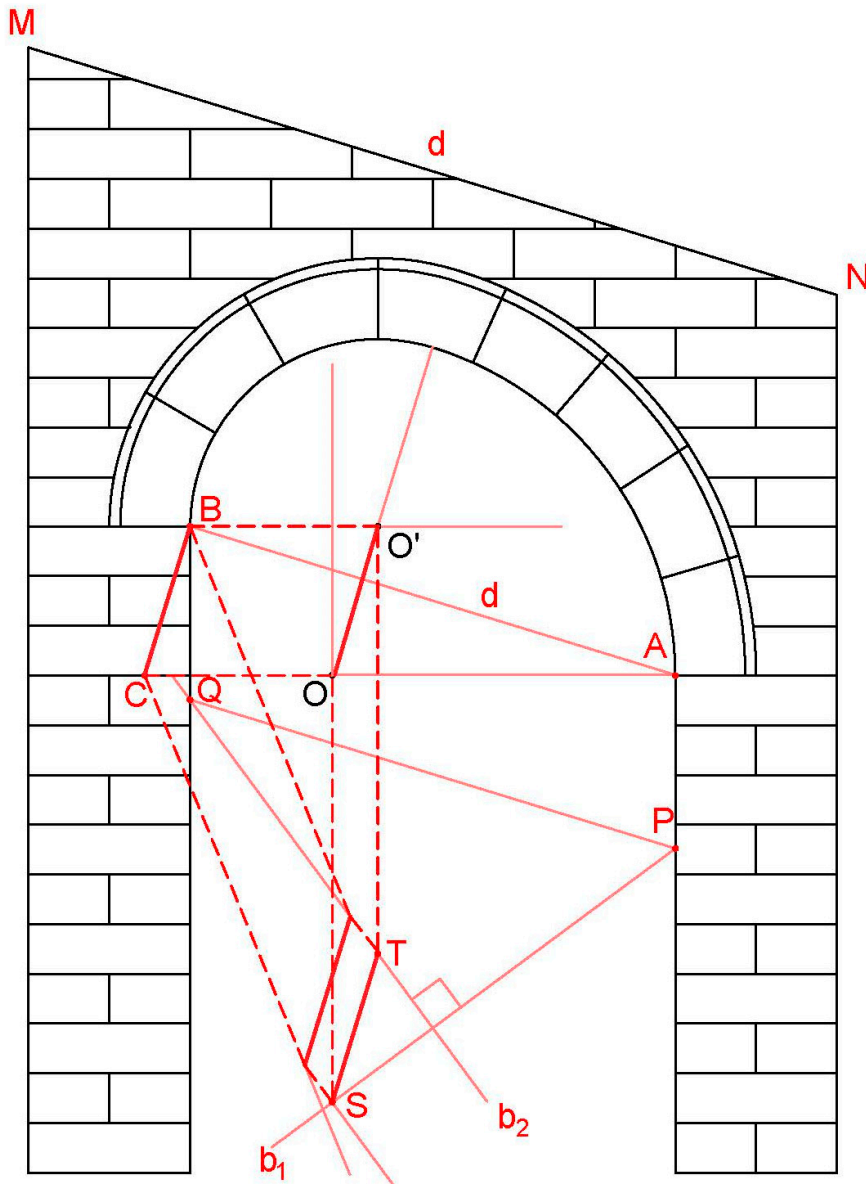

Figure 7. Graphical design of the optimal rampant arch.

3.2. Analytical Calculation

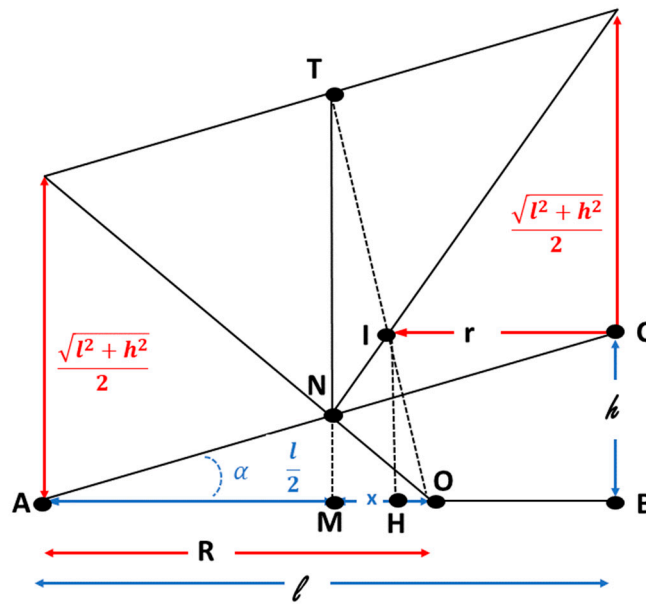For the mathematical deduction, the scheme of Figure 8 was followed.

Figure 8. Geometric elements to define the optimal rampant arch.

This scheme traces a rampant arch any ATC, of span l and rise h where the following relationships exist:

$$AB = l,$$

$$BC = HI = h,$$

$$OA = OT = R,$$

$$IC = HB = r,$$

$$OI = R - r.$$

In the triangle OMN,

$$\tan \alpha = \frac{\frac{h}{2}}{R - \frac{l}{2}} = \frac{h}{2R - l}.$$

In the triangle IHO,

$$\sin 2\,\alpha = \frac{h}{R - r};$$

therefore, it is

$$2R - l = \frac{h\,\cos \alpha}{\sin \alpha},$$

$$2R - 2r = \frac{h}{\sin \alpha \cos \alpha},$$

where

$$2r - l = \frac{h\left(\cos^2 \alpha - 1\right)}{\sin \alpha\,\cos \alpha} = -\frac{h \sin \alpha}{\cos \alpha}.$$

Then, we get

$$2R = l + \frac{h\,\cos \alpha}{\sin \alpha},$$

$$2r = l - \frac{h \sin \alpha}{\cos \alpha},$$

$$\frac{R}{r} = \frac{\frac{l\sin \alpha\, +h\cos \alpha\,\infty}{\sin \alpha}}{\frac{l\cos \alpha - h\sin \alpha}{\cos \alpha}} = \frac{l\sin \alpha \cos \alpha + h\cos^2 \alpha}{l\sin \alpha\,\cos \alpha - h\sin^2 \alpha\,\infty} = \frac{\frac{l\sin 2\,\alpha}{2} + \frac{h(1+\cos 2\,\alpha)}{2}}{\frac{l\sin 2\,\alpha}{2} - \frac{h(1-\cos 2\,\alpha)}{2}} = \frac{l\sin 2 \propto +h\cos 2\,\alpha + h}{l\sin 2\,\alpha + h\cos 2\,\alpha - h}.$$

That is to say, in short,

$$\frac{R}{r} = 1 + \frac{2h}{l \sin 2 \propto + h \cos 2 \propto - h},$$

deriving

$$\left(\frac{R}{r}\right)' = \frac{2h \left(2l \cos 2\,\alpha - 2h \sin 2\,\alpha\right)}{\left(l \sin 2\,\alpha + h \cos 2\,\alpha - h\right)^2} = 0,$$

$$\cot 2\,\alpha = \frac{h}{l}.$$

In other words, the optimum rampant arch is the one with the tangent parallel to the uneven line.

The relationship between the radii of curvature in a rampant arch will be found when the tangent is parallel to the straight line of unevenness. Let l the distance between walls (span) and h be the rise. One has, by resemblance of triangles,

$$R = \frac{l}{2} + x,$$

$$R.r = \frac{l^2 + h^2}{4},$$

$$\frac{\sqrt{l^2 + h^2}}{2} = \frac{\frac{h}{2}}{x},$$

where

$$x = \frac{lh}{2} \frac{1}{\left(\sqrt{l^2 + h^2}\right) - h},$$

and

$$R = \frac{l}{2} \left|1 + \frac{h}{\left(\sqrt{l^2 + h^2}\right) - h}\right| = \frac{l^2 + h^2 + h\sqrt{l^2 + h^2}}{2l};$$

Therefore,

$$r = \frac{l^2 + h^2}{4R} = \frac{\frac{l^2 + h^2}{2\left(l^2 + h^2 + h\sqrt{l^2 + h^2}\right)}}{l} = \frac{\left(\sqrt{l^2 + h^2}\right)l}{2\left(\sqrt{l^2 + h^2} + h\right)},$$

where

$$\frac{R}{r} = \frac{\left(\sqrt{l^2 + h^2} + h\right)^2}{l^2}.$$

Dividing by l^2 numerator and denominator and calling $\frac{h}{l} = p$; then $\frac{R}{r} = \left(\sqrt{1 + p^2} + p\right)^2$. If we call $\frac{R}{r} = k$, it results in $p = \frac{k-1}{2\sqrt{k}}$.

3.3. Computer Software

The above calculus was programmed in MATLAB. Figure 9 shows the programming diagram, with the calculations described in the previous section. The program can calculate the arcs either analytically, by entering the coordinates of the starting and ending points, or graphically, on a scaled image. In Figure 10, several examples of rampant arch calculations are shown, where the coordinates of the start and end points were entered. Note that they are shown in blue on the graph obtained (Figure 10A). In the first example, the coordinates were for the initial point (1, 1), and for the final point (3, 3), so that the horizontal separation or span (l) between both was 2 m and the vertical or rise (h) was also 2 m, obtaining the coordinates of the center of the major arch (5, 1) and those of the minor arch (2.33, 3). In Figure 10B, an example of calculation of rampant arches in stairs is shown, where the two circumferences and their radii are highlighted.
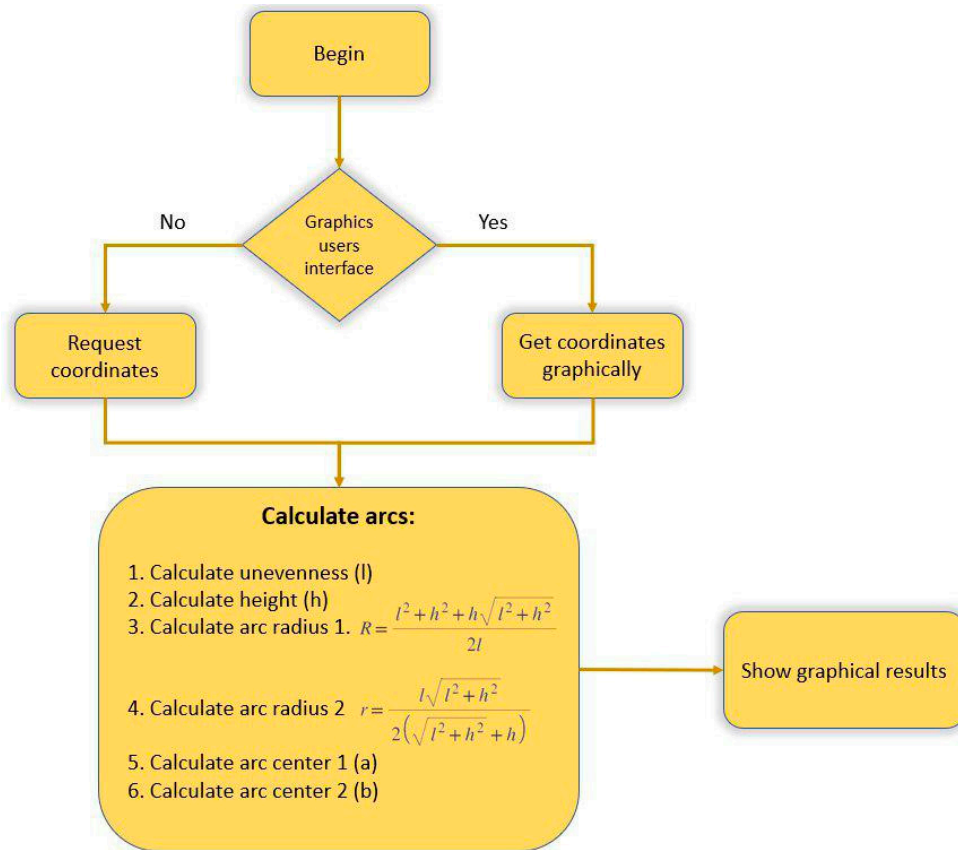
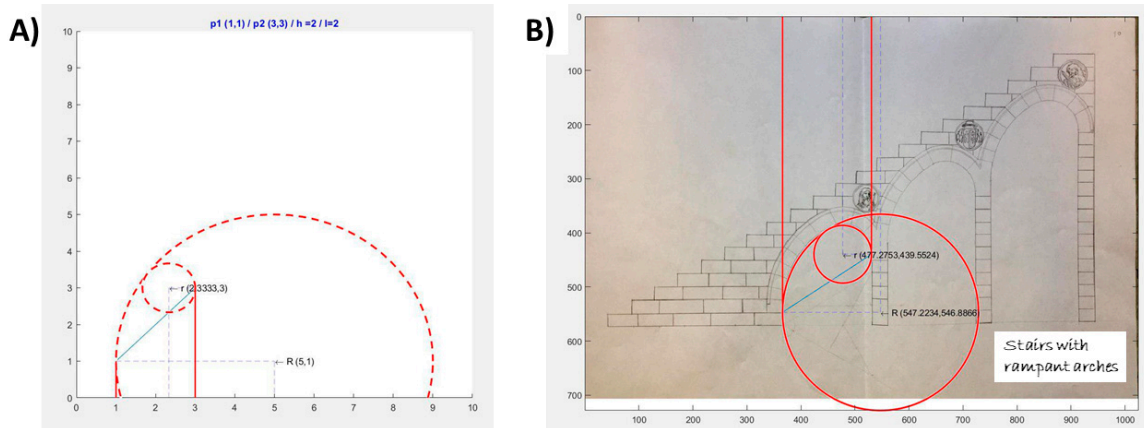**Figure 9.** Software calculation diagram for optimal rampant arch calculation.

Figure 10. Rampant arches with different geometries: (**A**) numerical data input; (**B**) graphical data input.

4. Case Studies

In this section, two case studies of real rampant arches were selected, representative cases of Gothic art in France (church of Saint Urbain de Troyes) and Spain (Cathedral of Palma de Mallorca), where one comes out as an optimal rampant arch and the other does not.

4.1. Church of Saint Urbain de Troyes (France)

The Saint Urban Church (Église Saint-Urbain) is a large medieval French church erected in the city of Troyes, now the capital of the department of Aube. It was a collegiate church, endowed in 1262 by Pope Urban IV, and it is a remarkable example of late Gothic architecture. Construction of the building probably began in 1263, where the main section of the church was not completed until the

16th century, and the tower was not completed until 1630. One of its highlights is the collegiate choir, long acclaimed as a masterpiece of French Gothic architecture, and demonstrates the advanced degree of sophistication of French architecture in the third quarter of the 13th century [25,26]. This church was the object of numerous architectural studies as an example of the French Gothic style [13]. Figure 11 shows the calculation of the optimum rampant arch calculated with the software overlapped over the original arch of the Church of Saint Urbain de Troyes. The starting (A) and ending (C) points are marked in the section of the rampant arch. Note that the actual arch is far from the optimal rampant arch calculated with the software.
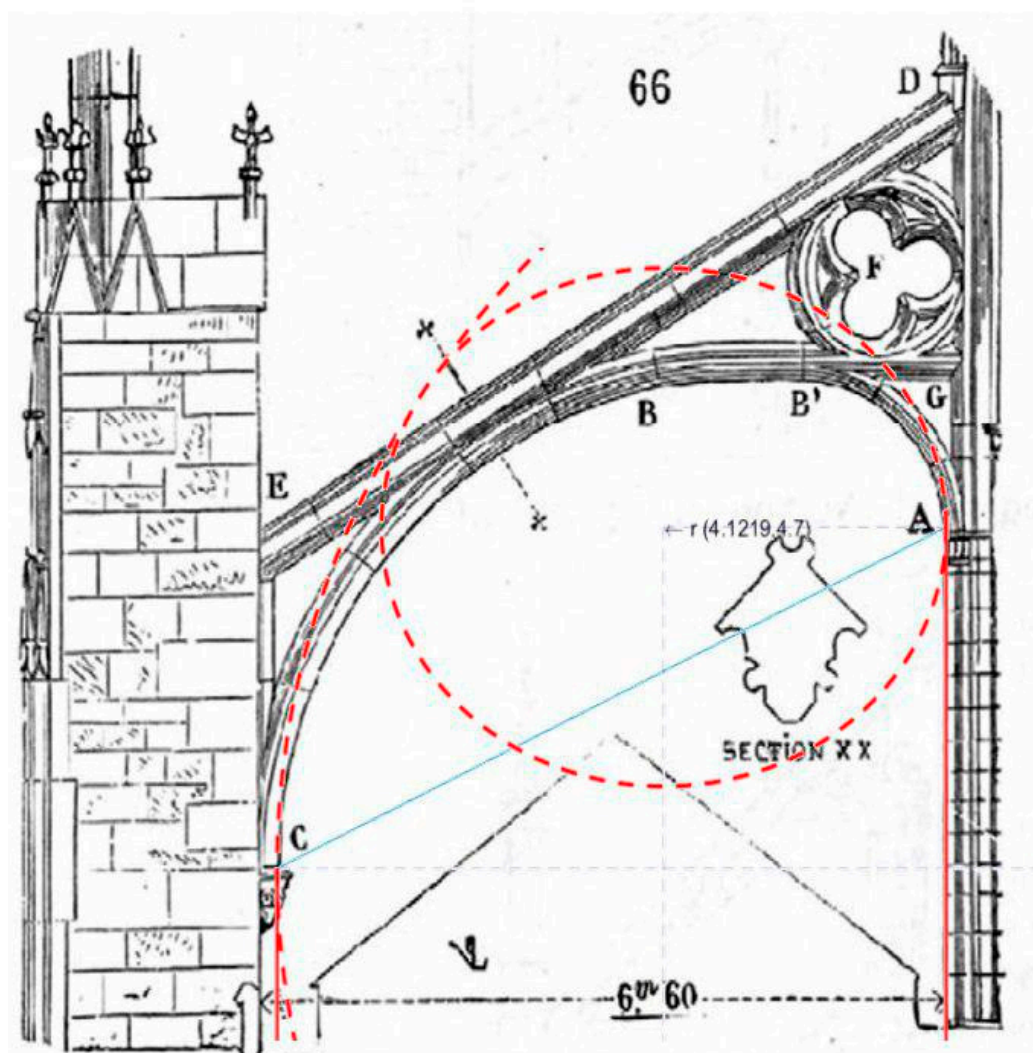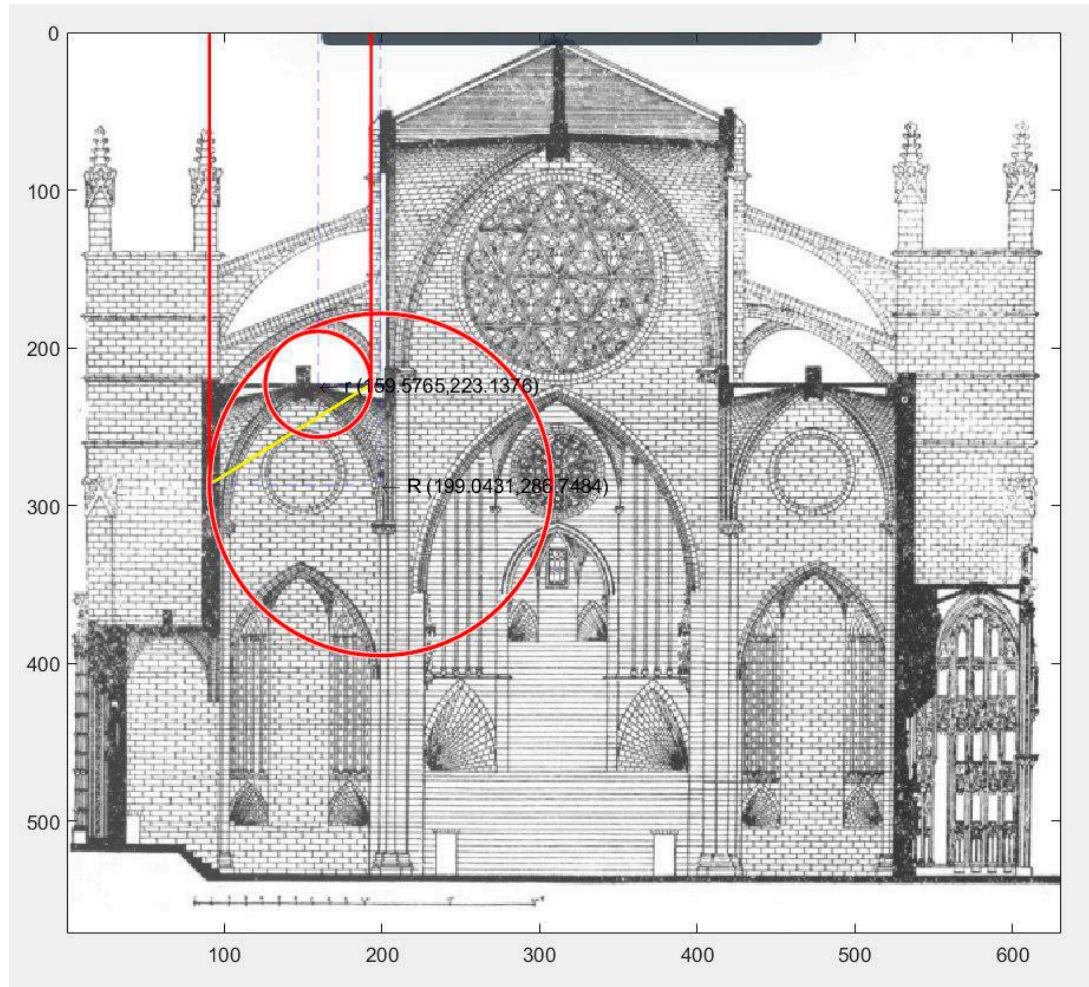

Figure 11. Calculation of the optimal rampant arch (in red) over a rampant arch of the flying buttress of the church of Saint Urbain de Troyes (France).

4.2. Cathedral of Palma de Mallorca (Spain)

The Cathedral-Basilica of Santa María de Palma de Mallorca, also known as the Cathedral of Mallorca, is one of the most significant monuments of Spanish Gothic architecture [27]. Its construction started around the year 1300 and was completed around the year 1600 [28]. Its vault reaches a height of 44 m, only surpassed by the Cathedral of Beauvais (48 m), the highest Gothic cathedral in the world, and slightly lower than the height of the Cathedral of Milan (45 m). Moreover, it surpasses the Cathedral of Cologne 43 m, and it is, therefore, considered as one of those with a nave of greater height among the cathedrals of European Gothic style [29]. In Figure 12, the optimal rampant arch was calculated on one of the arches of the façade of the cathedral of Palma de Mallorca. Here, you can

see how the arch calculated with the software and the real arch match. Indeed, a recent study on the structure of the cathedral of Palma de Mallorca showed the horizontal displacements of the façade [27], where it was observed that the rampant arches do not have any displacement, as a result of its proper construction and design.

Figure 12. Calculation of the optimal rampant arch over a flying buttress (in red) of the Cathedral of Palma de Mallorca (Spain). Note that the yellow line highlights the initial and final points of the rampant arch.

5. Discussion

In Gothic constructions, the flying buttresses of the first constructions were generally circular, where the shape of the line of thrust did not match, normally, with the geometric forms of traditional construction formed by circumferential arches [4]. In addition, when the line of thrust reaches or touches the edge of the arch, an articulation is formed that can cause the arch to collapse [21]. Enough arch thickness will easily accommodate an infinite number of thrust lines. By progressively reducing the thickness of the arch, the moment will come when there will be only one line of thrusts and the thickness of the arch cannot be reduced without it exiting the line of the arch. Note that load-bearing structures in Gothic cathedrals account for 85% to 90% of the building material [30]. Therefore, the design of the rampant arches of two arches tried lightening the structure while maintaining or improving the thrust resistance of the flying buttresses.

In general, the only action to be considered in constructions made with ashlars, such as Gothic cathedrals, is the position of the line of thrusts by its own weight. Scientific calculation, therefore, justifies the use of geometric or graphical patterns. Therefore, the ancient builders understood

the essence of building with ashlars: the proper placement of weights, the balance of thrusts, and counterbalances. This knowledge of the decisive importance of geometry is perhaps the secret of Gothic constructions. In this research, it was shown how the rampant arches of cathedrals like the Palma de Mallorca are optimum from the geometric point of view.

This work may have limitations from a practical point of view. Firstly, if it is analyzed numerically, the precision of the calculation of centers and radii will depend on the precision of the coordinates of the starting and finishing points of the arc. Secondly, from the point of view of analyzing existing constructions, historical plans were analyzed to scale, which are not always available, and can sometimes have distortions or errors [31–33].

In order to analyze real existing cases, a centimetric precision survey would be needed. Although, currently, with the technology of unmanned aerial vehicles, it could be solved in a relatively economic way by realizing a photogrammetric survey [34]. In the literature, several examples can be found [35,36].

On the other hand, if the rampant arches to be analyzed are close to the ground, such as those commented on for staircases or inside buildings, other techniques can be used, such as close-range photogrammetry [37–39] or terrestrial laser scanning [40].

6. Conclusions

In this work, the geometry of the rampant arch was studied from different approaches, the graphical point of view known in classical literature and the current mathematical point of view, with its subsequent programming. An optimal geometrical solution was defined from the constructive point of view and was calculated and programmed. The optimum rampant arch obtained is the one with the common tangent to the two arches parallel to the slope line. Additionally, knowing the radii of the two arcs, the software allows calculating the starting points of both arches on the pillars or walls. It was applied to several well-known and representative cases of Gothic art in France (church of Saint Urbain de Troyes) and Spain (Cathedral of Palma de Mallorca), establishing that the first was not an optimal design while the second was. The conception and study of certain architectural elements, such as the rampant arch, not only help identify and describe existing aspects of our traditional architecture, but can also serve as a starting point for the verification of existing structures, which, despite standing for many years, may require intervention. This research opens new perspectives for the geometric study of buttresses of cathedrals in general and of rampant arches in particular. It was possible to analyze the geometries used in the design of cathedrals, and specifically through the proposed case studies. It was verified how the constructors reached the optimum rampant arch from a structural point of view, defined as the one whose tangent between the two arches is parallel to the straight unevenness between the initial and final points of the rampant arch.

Author Contributions: C.V., A.A., C.S.-A.-G., F.G.M., I.Z., and F.M.-A. conceived the study, designed the method, and wrote the manuscript.

Conflicts of Interest: The authors declare no conflict of interest.

References

1. Warland, E.G. *Modern Practical Masonry*; Routledge: Abingdon-on-Thames, UK, 2006. [CrossRef]
2. Theodossopoulos, D. Structural scheme of the Cathedral of Burgos. *Struct. Anal. Hist. Constr.* **2004**, *4*, 643–652.
3. Sánchez-Beitia, S. On-site Stress Measurements of a Flying Buttress in the Palma de Mallorca (Spain) Cathedral. *Rock Mech. Rock Eng.* **2016**, *49*, 315–319. [CrossRef]
4. Llopis-Pulido, V.; Durá, A.A.; Fenollosa, E.; Martínez, A. Analysis of the Structural Behavior of the Historical Constructions: Seismic Evaluation of the Cathedral of Valencia (Spain). *Int. J. Archit. Herit.* **2019**, *13*, 205–214. [CrossRef]

5. Viollet le Duc, E. Dictionnaire Raisonné de L'architecture Française du XIe au XVIe Siècle. B. Bance, París. 1854. Available online: https://fr.wikisource.org/wiki/Livre:Viollet-le-Duc_-_Dictionnaire_raisonn%C3%A9_de_l%E2%80%99architecture_fran%C3%A7aise_du_XIe_au_XVIe_si%C3%A8cle,_1854-1868,_tome_1.djvu (accessed on 15 April 2019).

6. Tarrío, I. Los arbotantes en el sistema de contrarresto de construcciones medievales: Teorías sobre su comportamiento estructural. In *Actas del IX Congreso Nacional y I Internacional Hispanoamericano de Historia de la Construcción*; Instituto Juan de Herrera: Madrid, Spain, 2015; Volume 3, p. 1677.

7. Deio, G. Durham Cathedral Plans. Available online: https://www.medart.pitt.edu/image/england/Durham/Cathedral/Plans/dc149dur-b.jpg (accessed on 15 April 2019).

8. Choisy, A. *Histoire de L'architecture Tome II*; Beránger, G., Ed.; Gauthier-Villars: Paris, France, 1899.

9. Courtenay, L.T. *The Engineering of Medieval Cathedrals*; Routledge: Abingdon-on-Thames, UK, 2016. [CrossRef]

10. Moya, D. *El Origen de los Arbotantes en la Historia de la Arquitectura, X Certamen Arquímedes de Introducción a la Investigación Científica*; Ministerio de Educación y CSIC: Madrid, Spain, 2011; p. 2.

11. Tempesta, G.; Galassi, S. Safety evaluation of masonry arches. A numerical procedure based on the thrust line closest to the geometrical axis. *Int. J. Mech. Sci.* **2019**, *155*, 206–221. [CrossRef]

12. Panofsky, E. *Gothic and Architecture and Scholasticism*; Archabbey Press: New York, NY, USA, 1957; ISBN 0529020920.

13. Davis, M.T.; Neagley, L.E. Mechanics and Meaning: Plan Design at Saint-Urbain, Troyes and Saint-Ouen, Rouen. *Gesta* **2000**, *39*, 161–182. [CrossRef]

14. Heyman, J. Beauvais cathedral. *Trans. Newcom. Soc.* **1967**, *40*, 15–35. [CrossRef]

15. Pelà, L.; Bourgeois, J.; Roca, P.; Cervera, M.; Chiumenti, M. Analysis of the effect of provisional ties on the construction and current deformation of Mallorca Cathedral. *Int. J. Archit. Herit.* **2016**, *10*, 418–437. [CrossRef]

16. Derand, F. L'Architecture des Voutes, ou l'art, traits et coupes des voutes; traite tres-utile, méme nécessaire à tous les architectes, maitres-maçons, appareilleurs, tailleurs de pierres, et généralement à tous ceux qui se mélent de l'Architecture, meme militaire, París: S. Cramoysi, 1643. Available online: https://gallica.bnf.fr/ark:/12148/btv1b8626566f/f7.image (accessed on 24 April 2019).

17. Blondel, F.N. Cours d' Architecture enseigné dans l'Académie royale d' architecture. Ed. P. Auboin et F. Clouzier (Paris). 1675. Available online: https://gallica.bnf.fr/ark:/12148/bpt6k85661p.r=cours%20architecture%20cours%20architecture?rk=21459;2 (accessed on 24 April 2019).

18. Casado, E.A.; Sánchez, J.M.D. Geometría del arco carpanel. *Suma: Revista sobre Enseñanza y Aprendizaje de las Matemáticas* **2015**, *79*, 17–25.

19. Quintas, V. Structural analysis of flying buttresses. *Eur. J. Environ. Civ. Eng.* **2017**, *21*, 471–507. [CrossRef]

20. Portioli, F.; Cascini, L.; Casapulla, C.; D'Aniello, M. Limit analysis of masonry walls by rigid block modelling with cracking units and cohesive joints using linear programming. *Eng. Struct.* **2013**, *57*, 232–247. [CrossRef]

21. Frezier, A.F. La Théorie et la Pratique de la Coupe des Pierres et des Bois pour la Construction des Voûtes et Autres Parties des Bâtiments Civils & Militaires, ou Traité de Stéréotomie, à L'usage de L'architecture. Tome 3. Strasbourg and Paris (1737-9). Available online: https://gallica.bnf.fr/ark:/12148/bpt6k1040142z/f491.image (accessed on 15 April 2019).

22. Breymann, G.U. Bau-Constructions-Lehre. Berlag von Gustav Beise. 1881. Available online: https://www.e-rara.ch/zut/content/pageview/8642945 (accessed on 15 April 2019).

23. Heyman, J. The stone skeleton. *Int. J. Solids Struct.* **1966**, *2*, 249–279. [CrossRef]

24. Theodossopoulos, D.; Sinha, B.P.; Usmani, A.S. Case study of the failure of a cross vault: Church of Holyrood Abbey. *J. Archit. Eng.* **2003**, *9*, 109–117. [CrossRef]

25. Bruzelius, C. The Second Campaign at Saint-Urbain at Troyes. *Speculum* **1987**, *62*, 635–640. [CrossRef]

26. Davis, M.T. On the Threshold of the Flamboyant: The Second Campaign of Construction of Saint-Urbain, Troyes. *Speculum* **1984**, *59*, 847–884. [CrossRef]

27. Roca, P.; Cervera, M.; Pelà, L.; Clemente, R.; Chiumenti, M. Continuum FE models for the analysis of Mallorca Cathedral. *Eng. Struct.* **2013**, *46*, 653–670. [CrossRef]

28. Elyamani, A.; Roca, P.; Caselles, O.; Clapes, J. Seismic safety assessment of historical structures using updated numerical models: The case of Mallorca cathedral in Spain. *Eng. Fail. Anal.* **2017**, *74*, 54–79. [CrossRef]

29. Pérez-Gracia, V.; Caselles, J.O.; Clapés, J.; Martinez, G.; Osorio, R. Non-destructive analysis in cultural heritage buildings: Evaluating the Mallorca cathedral supporting structures. *NDT E Int.* **2013**, *59*, 40–47. [CrossRef]

30. Fitchen, J. *The Construction of Gothic Cathedrals: A Study of Medieval Vault Erection*; University of Chicago Press: Chicago, IL, USA, 1981.

31. San-Antonio-Gómez, C.; Velilla, C.; Manzano-Agugliaro, F. Photogrammetric techniques and surveying applied to historical map analysis. *Surv. Rev.* **2015**, *47*, 115–128. [CrossRef]

32. Manzano-Agugliaro, F.; Montoya, F.G.; San-Antonio-Gómez, C.; López-Márquez, S.; Aguilera, M.J.; Gil, C. The assessment of evolutionary algorithms for analyzing the positional accuracy and uncertainty of maps. *Expert Syst. Appl.* **2014**, *41*, 6346–6360. [CrossRef]

33. San-Antonio-Gómez, C.; Velilla, C.; Manzano-Agugliaro, F. Urban and landscape changes through historical maps: The Real Sitio of Aranjuez (1775–2005), a case study. *Comput. Environ. Urban Syst.* **2014**, *44*, 47–58. [CrossRef]

34. Perea-Moreno, A.J.; Aguilera-Ureña, M.J.; Larriva, M.D.; Manzano-Agugliaro, F. Assessment of the potential of UAV video image analysis for planning irrigation needs of golf courses. *Water* **2016**, *8*, 584. [CrossRef]

35. Achille, C.; Adami, A.; Chiarini, S.; Cremonesi, S.; Fassi, F.; Fregonese, L.; Taffurelli, L. UAV-based photogrammetry and integrated technologies for architectural applications—Methodological strategies for the after-quake survey of vertical structures in Mantua (Italy). *Sensors* **2015**, *15*, 15520–15539. [CrossRef] [PubMed]

36. Karachaliou, E.; Georgiou, E.; Psaltis, D.; Stylianidis, E. Uav for Mapping Historic Buildings: From 3d Modelling to Bim. In *International Archives of the Photogrammetry, Remote Sensing and Spatial Information Sciences, Proceedings of the 8th International Workshop 3D-ARCH "3D Virtual Reconstruction and Visualization of Complex Architectures", Bergamo, Italy, 6–8 February 2019*; International Society of Photogrammetry and Remote Sensing (ISPRS): Hannover, Germany, 2019.

37. Yilmaz, H.M.; Yakar, M.; Gulec, S.A.; Dulgerler, O.N. Importance of digital close-range photogrammetry in documentation of cultural heritage. *J. Cult. Herit.* **2007**, *8*, 428–433. [CrossRef]

38. Jiang, R.; Jáuregui, D.V.; White, K.R. Close-range photogrammetry applications in bridge measurement: Literature review. *Measurement* **2008**, *41*, 823–834. [CrossRef]

39. Grussenmeyer, P.; Landes, T.; Voegtle, T.; Ringle, K. Comparison methods of terrestrial laser scanning, photogrammetry and tacheometry data for recording of cultural heritage buildings. *Int. Arch. Photogramm. Remote Sens. Spat. Inf. Sci.* **2008**, *37*, 213–218.

40. Lerma, J.L.; Navarro, S.; Cabrelles, M.; Villaverde, V. Terrestrial laser scanning and close range photogrammetry for 3D archaeological documentation: The Upper Palaeolithic Cave of Parpalló as a case study. *J. Archaeol. Sci.* **2010**, *37*, 499–507. [CrossRef]